

We are IntechOpen, the world's leading publisher of Open Access books Built by scientists, for scientists

4,800

Open access books available

122,000

International authors and editors

135M

Downloads

Our authors are among the

154

Countries delivered to

TOP 1%

most cited scientists

12.2%

Contributors from top 500 universities



WEB OF SCIENCE™

Selection of our books indexed in the Book Citation Index
in Web of Science™ Core Collection (BKCI)

Interested in publishing with us?
Contact book.department@intechopen.com

Numbers displayed above are based on latest data collected.
For more information visit www.intechopen.com



CFD Application for Gas Turbine Combustion Simulations

*Valeriu Vilag, Jeni Vilag, Razvan Carlanescu,
Andreea Mangra and Florin Florean*

Abstract

The current chapter presents the use of computational fluid dynamics (CFD) for simulating the combustion process taking place in gas turbines. The chapter is based on examples and results from a series of applications developed as part of the research performed by the authors in national and European projects. There are envisaged topics like flame stability, pollutant emission prediction, and alternative fuels in the context of aviation and industrial gas turbines, growing demands for lower fuel consumption, lower emissions, and overall sustainability of such energetic machines. Details on the available numerical models and computational tools are given along with the expectation for further developing CFD techniques in the field. The chapter includes also some comparison between theoretical, numerical, and experimental results.

Keywords: combustion, gas turbine, numerical simulations, models, alternative fuels, experiments

1. Introduction

Gas turbines are energetic machines based on Brayton thermodynamic cycle [1] (**Figure 1**) meaning, among others, temperature rise using combustion at quasi-constant pressure.

In **Figure 1**, evolution (1–2) represents the real compression evolution of the working fluid into the compressor, (2–3) represents combustion at constant pressure, (3–4) represents real expansion of the working fluid into the turbine, and (4–1) represents the cooling down of the working fluid at constant pressure, usually the atmospheric one. Evolutions (1–2_{is}) and (3–4_{is}) are the isentropic compression and isentropic expansion, respectively, and they are shown on the graphic in order to emphasize the difference between real and ideal (isentropic).

Unlike compressors and turbines in which only pure gas-dynamic processes develop, combustion involves also chemical reactions between air and fuel, resulting in flue gases driving the turbine. Since combustion is known from ages, the overall efficiency of it is very high [2] and enhanced by the high pressure provided by the compressor. Still, many current studies are directed on this subject willing to reduce pollutant emissions or to accommodate alternative fuels such as biogas or both.

In general, the combustion process is organized into the gas turbine as shown in **Figure 2** [3].

In **Figure 2** the red arrows represent the burning working fluid (realizing close to stoichiometric mixture ratio with the injected fuel and very high temperature in the flame presented in orange), and the blue arrows represent the fluid which cools down the burning one down to the required temperature of the thermodynamic cycle (which is limited by the materials used to realize the combustion chamber and the turbine).

The arrangement of the combustion chamber is the subject of many research projects, some of the latest being lean burn program [4] where the reduction of NO_x through the reduction of combustion temperature by multiple combustion is sought.

In **Figure 3**, depicted is a type of combustion which may lead to lower NO_x production: the red zone (R) is rich in fuels, meaning more fuel than the calculated

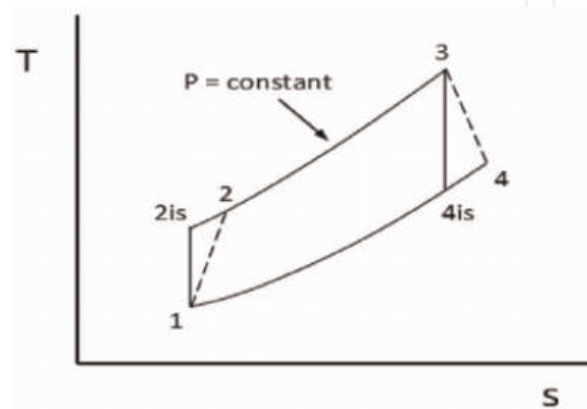


Figure 1.
Brayton cycle in temperature vs. entropy coordinates.

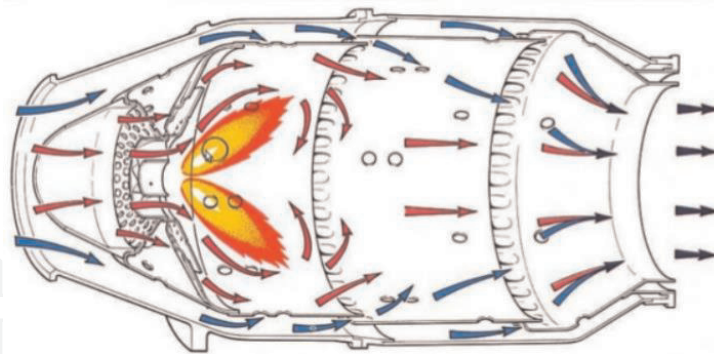


Figure 2.
Combustion chamber.

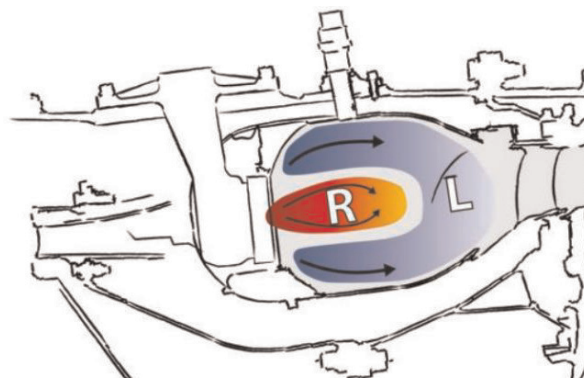
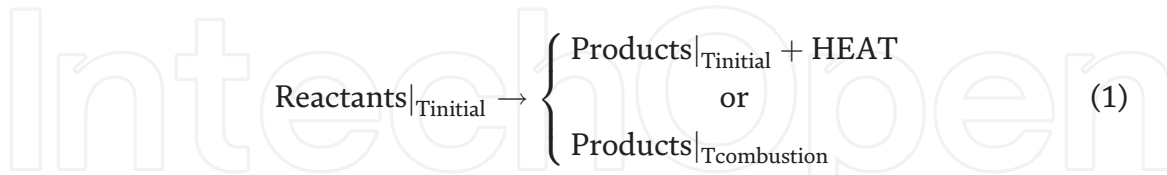


Figure 3.
Clean Sky research project [4].

from stoichiometric reaction, while the blue zone (L) is lean in fuel, meaning less fuel than the calculated from stoichiometric reaction. The Clean Sky research project aims at demonstrating that by realizing such an arrangement of the combustion process, the maximum flame temperature can be lowered reducing thus the dissociation reactions that create NO_x, at the same final temperature reaching the turbine.

The thermodynamics of combustion is relatively simple and is based on the heat of reaction as shown in Eq. (1):



Still, the use of this equation gives good results only for the temperature at the end of the combustion process and not so accurate results on the resulting composition. Thus, the chemical reaction must be carefully studied and implemented in the study concerning the combustion chamber of a gas turbine.

Computational fluid dynamics (CFD) has been intensively used in the aerospace domain mainly for predicting the performances of the studied object which can be the entire aircraft or some particular part of it. For the gas turbines, all the main components can be studied using CFD: in the case of the compressor, the aerodynamic part is the most important seeking for high efficiency of transforming the available mechanical work into total pressure of the air; in the case of the turbine, the things are reversed, the study being focused on reducing the losses of transforming the potential energy of the fluid in the form of pressure and temperature, into mechanical work; in the case of the combustion chamber, aerodynamics plays a big role in the injection of fuel and mixing, but it must be coupled with chemical reactions and heat release within the transforming fluid.

2. Combustion and chemistry in CFD

The combustion process is the result of a strong exothermic chemical reaction as a result of energy exchanges that occur due to intermolecular collisions.

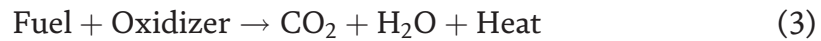
Generally, at ambient temperature, a chemical reaction occurs very slowly, because, although collisions at molecular level occur, they do not generate a sufficient amount of energy to trigger a chemical transformation.

According to the chemical kinetic theory, only “active” collisions, collisions involving molecules having an initial energy greater than or equal to an energy called activation energy, lead to a chemical reaction. This energy is needed to destroy or weaken existing intermolecular connections. The activation energy is given by Arrhenius equation [5, 6]:

$$k = A \cdot T^{\beta} \cdot \exp\left(\frac{-E_a}{R \cdot T}\right) \quad (2)$$

where k is the reaction rate coefficient, A is the pre-exponential factor, E_a is the activation energy, R is the universal gas constant, β is the temperature exponent, and T is the temperature.

The combustion process can be expressed in a simplified way through the global reaction mechanism, Eq. (3):



In CFD modeling more complex reaction mechanisms (e.g., mechanisms which take into consideration the formation of NO) are also available. Using a more complex reaction mechanism is more time-consuming and requires higher computational power. Thus, depending on the purpose of the conducted numerical simulation, a simpler or more complex reaction mechanism should be chosen.

In CFD modeling several combustion models are available [7–9].

2.1 Eddy dissipation model (EDM)

The eddy dissipation model is based on the concept that chemical reaction is fast relative to the transport processes in the flow. When reactants mix at the molecular level, they instantaneously form products. The model assumes that the reaction rate may be related directly to the time required to mix reactants at the molecular level.

By default, for the eddy dissipation model, it is sufficient that fuel and oxidant be available in the control volume for combustion to occur.

Because of the assumption of complete combustion, the eddy dissipation model may overpredict temperature under certain conditions (e.g., for hydrocarbon fuels in regions with fuel-rich mixture).

The eddy dissipation model was developed for use in a wide range of turbulent reacting flows covering premixed and diffusion flames. Because of its simplicity and robust performance in predicting turbulent reacting flows, this model has been widely applied in the prediction of industrial flames.

2.2 The finite-rate chemistry (FRC) model

The finite-rate chemistry model allows the computation of reaction rates described by the molecular interaction between the components in the fluid. It can be combined with the eddy dissipation model for flames where chemical reaction rates might be slow compared with the reactant mixing rates. The finite-rate chemistry model is best applied to situations where the chemical time scale is rate-limiting. This model can be used in conjunction with both laminar and turbulent flow.

2.3 The flamelet model

The flamelet model can provide information on minor species and radicals, such as CO and OH, and accounts for turbulent fluctuations in temperature and local extinction at high scalar dissipation rates, for the cost of solving only two transport equations. The model is only applicable for two-feed systems (fuel and oxidizer) and requires a chemistry library as input. The model can be used only for non-premixed systems.

The flamelet concept for non-premixed combustion describes the interaction of chemistry with turbulence in the limit of fast reactions (large Damköhler number). The combustion is assumed to occur in thin sheets with inner structure called flamelets. The turbulent flame itself is treated as an ensemble of laminar flamelets which are embedded into the flow field.

The main advantage of the flamelet model is that even though detailed information of molecular transport processes and elementary kinetic reactions are included, the numerical resolution of small length and time scales is not necessary. This avoids the well-known problems of solving highly nonlinear kinetics in fluctuating flow fields and makes the method very robust. Only two scalar equations have to be solved independent of the number of chemical species involved in the simulation.

Information of laminar model flames are pre-calculated and stored in a library to reduce computational time (PDF table). On the other hand, the model is still restricted by assumptions like fast chemistry or the neglecting of different Lewis numbers of the chemical species.

The coupling of laminar chemistry with the fluctuating turbulent flow field is done by a statistical method. The PDF used can in principle be calculated at every point in the flow field by solving a PDF transport equation.

The most often mentioned advantage of this method is that the nonlinear chemical source term needs no modeling. Even though the method avoids some modeling which is necessary if using moment closure, it still requires modeling of some of the most important terms, in particular, the fluctuating pressure gradient term and the molecular diffusion term. If combustion occurs in thin layers as assumed here, the molecular diffusion term is closely coupled to the reaction term, and the problem of modeling the chemical source term is then shifted towards modeling the diffusion term.

2.4 Burning velocity model (BVM) and extended coherent flame model (ECFM)

The burning velocity model (BVM) and the extended coherent flame model (ECFM) model the propagation of a premixed or partially premixed flame by solving a scalar transport equation for the reaction progress. The BVM uses an algebraic correlation for modeling the turbulent burning velocity (propagation speed of the flame in turbulent flow). When using the ECFM, the turbulent burning velocity is closed by solving an additional transport equation for the flame surface density.

The BVM is a combined model using:

- A model for the progress of the global reaction: burning velocity model (BVM), also called turbulent flame closure (TFC).
- A model for the composition of the reacted and nonreacted fractions of the fluid: laminar flamelet with PDF.

The ECFM is a combined model employing:

- A model for the progress of the global reaction: extended coherent flame model (ECFM), which is a member of the class of flame surface density models.
- A model for the composition of the reacted and nonreacted fractions of the fluid: laminar flamelet with PDF.

2.5 The monotone integrated LES (MILES)

The model solves the unfiltered Navier-Stokes equations for a global chemical reaction mechanism. The method uses no sub-grid closure models but employs the inherent numerical scheme dissipation to account for the energy transferred to the sub-grid scales.

2.6 The linear eddy mixing (LEM) model

LEM is a stochastic approach aimed at stimulating the turbulent mixing, molecular diffusion, and the chemical reaction in a one-dimensional domain embedded in the LES cells of the computational domain (LEMLES). LEM is the only known

combustion model that does not use the scale separation hypothesis and is, therefore, valid even in regimes where the hypothesis fails. Also, the model is highly compatible with the large eddy simulation (LES) technique and very flexible in terms of the chemical reaction mechanism used to describe the chemical reactions. Nevertheless, the approach has some limitations. Most importantly, LEMLES is relatively much more expensive than conventional LES models, such as EBULES. However, it is highly scalable, so the overall computation time can be decreased by increasing the number of processors. Laminar molecular diffusion across LES cells is not included, but this limitation is significant only in laminar regions, whereas LEMLES is designed for high Reynolds number turbulent flow applications. Also, the viscous work is neglected in the sub-grid temperature equation but is explicitly included in the LES energy equation, which is used to ensure total energy conservation. Finally, the flame curvature effect is not explicitly present in the sub-grid.

3. CFD simulations for gas turbine combustion chamber and comparison to experimental results

3.1 Helicopter engine on alternative fuels

The desire to use top aviation technology in ground applications has led, through the years, to the transformation of a series of aviation gas turbines into drivers as part of industrial power plants. Some of these transformations have been made by the gas turbine producers, others even by beneficiaries or research institutions, such as COMOTI Romanian R&D Institute for Gas Turbines.

This section is focused on the behavior of a turboshaft with a structural construction allowing the modification of the entire fuel system, from the feeding lines, to the injection ramp and the actual injectors, as well as the relatively easy replacement of the aggregates.

From the theoretical point of view, several gaseous fuels have been studied as alternatives for the initial one, kerosene, such as methane and biogas with different chemical compositions (**Figure 4**). Obtaining chemical equilibrium for the

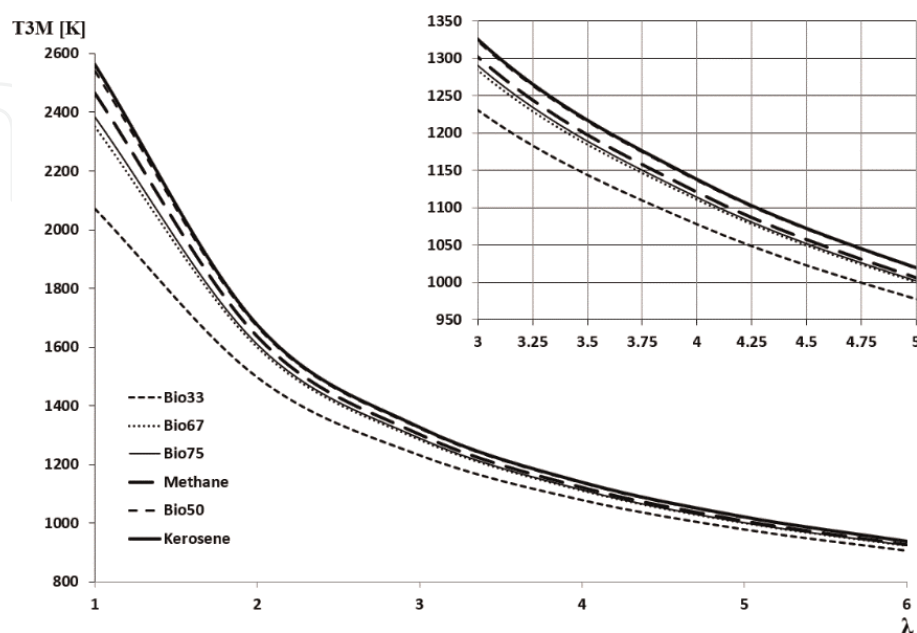


Figure 4. The variation of the combustion temperature (T_{3M}) with the air excess (λ) for different fuels (with focus on the usual zone for gas turbines).

combustion of these fuels has allowed to determine the parameters to be used as input data in numerical simulations of the combustion process in the gas turbine's combustor.

The numerical simulations, starting from data provided by either the producer, theoretical computations or experimental, include four cases, for the two mentioned alternative fuels, at two different operating regimes of the gas turbine: nominal and idle. The working fluids are defined as ideal gases: air as bicomponent mixture with 21% oxygen and 79% nitrogen; methane from the software library and biogas, as reacting mixture with 50% methane and 50% carbon dioxide. The cases are summarized in **Table 1**.

The numerical grid and boundary conditions are shown in **Figure 5**.

The eddy dissipation model, within ANSYS CFX [11], controls the formation of the reaction products, while the NO formation is controlled by two reaction schemes, WD1 and WDS. The advantage of the WDS scheme is that it also contains the CO creation model, through water-gas shift mechanism, allowing for higher accuracy, a fact also confirmed by the comparison with the experimental results, while the disadvantage consists in the necessity for higher computational resources and up to 50% more computing time. Some images with the temperature distribution in the combustion chamber are displayed in **Figures 6** and **7**.

Using the 17 double thermocouples mounted on the engine, **Figure 8** containing a comparison between numerical and experimental results was obtained. It can be seen that the numerical results predict that two areas of maximum temperature exist at the end of the combustion chamber, and it was confirmed by the experiments on the entire engine.

Case/ parameter	Reference pressure	Air mass flow rate	O ₂ mass fraction	Fuel mass flow rate	CH ₄ mass fraction	CO ₂ mass fraction
	[Pa]	[kg/s]		[kg/s]		
C1 Methane, nominal	760,000	0.825	0.233	0.010683	1	0
C2 Methane, idle	232,500	0.314	0.233	0.003212	1	0
C3 Biogas, nominal	760,000	0.825	0.233	0.0419	0.267	0.733
C4 Biogas, idle	232,500	0.314	0.233	0.0118	0.267	0.733

Table 1.
 Input data for numerical cases.

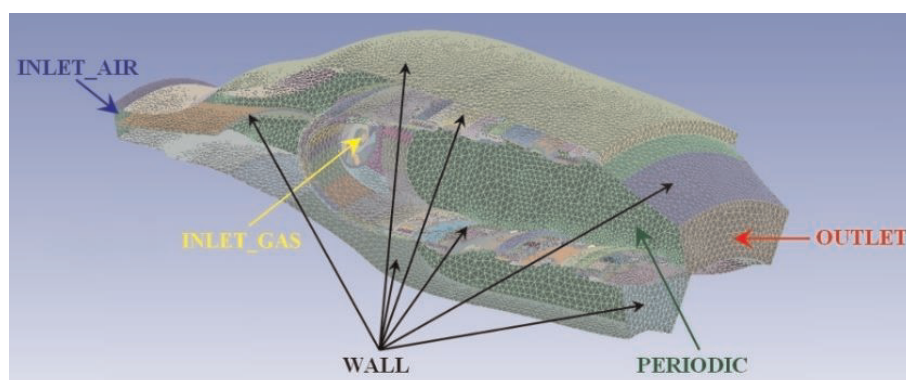


Figure 5.
 Computational grid with defined regions for the boundary conditions [10].

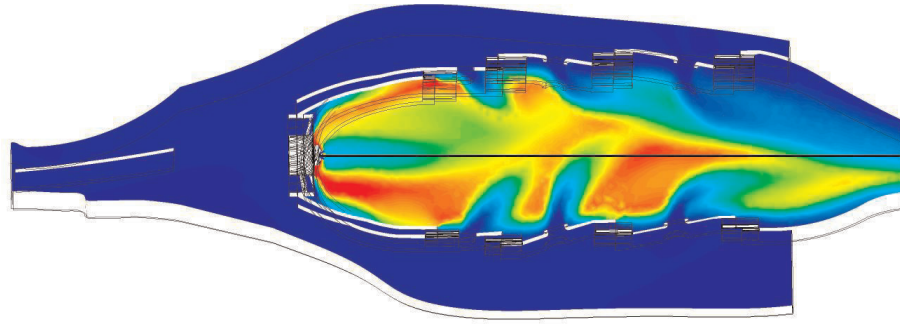


Figure 6.
General aspect of the temperature field in the combustor.

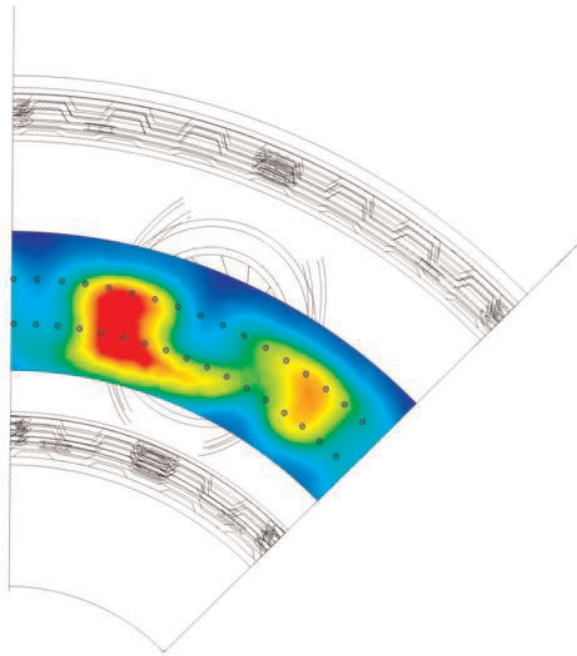


Figure 7.
Temperature fields at the end of the combustor.

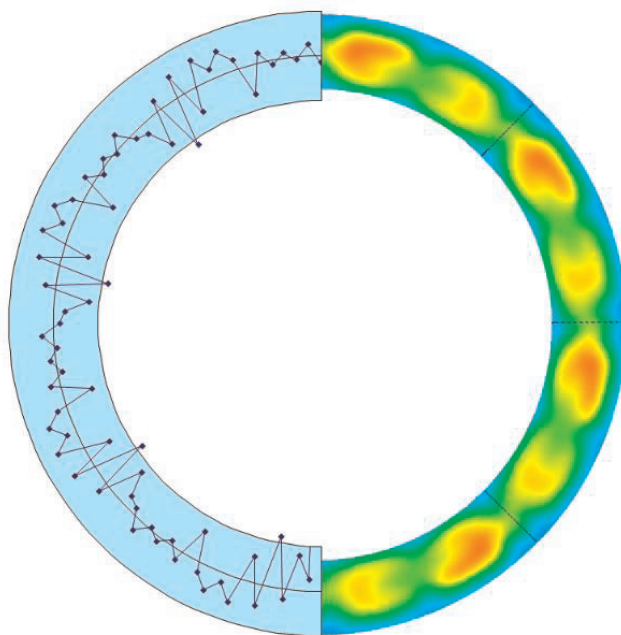


Figure 8.
Hybrid experimental diagram for biogas combustion [10].

3.2 Micro gas turbine for power generation

The numerical simulation of the gas-thermodynamic processes inside a Garrett micro gas turbine has been conducted using the commercial software ANSYS CFX. This work is part of the [12] PhD. thesis. The purpose of these numerical simulations was to validate the combination of numerical models used to simulate the turbulence process, combustion process, and liquid fuel atomization process and compare the numerical results with the functioning data of the used micro gas turbine engine.

The Garrett micro gas turbine is composed of an intake device, a single-stage centrifugal compressor, a tubular-type combustion chamber, a single-stage radial turbine, and an exhaust device (**Figure 9**).

The numerical simulation was performed only on the combustion chamber assembly. An unstructured-type computational grid, having 3.576.588 tetrahedral-type elements and 592.465 nodes, has been generated using ICEM CFD. A density was created near the injector to better capture the field near the fuel inlet (**Figure 10**).

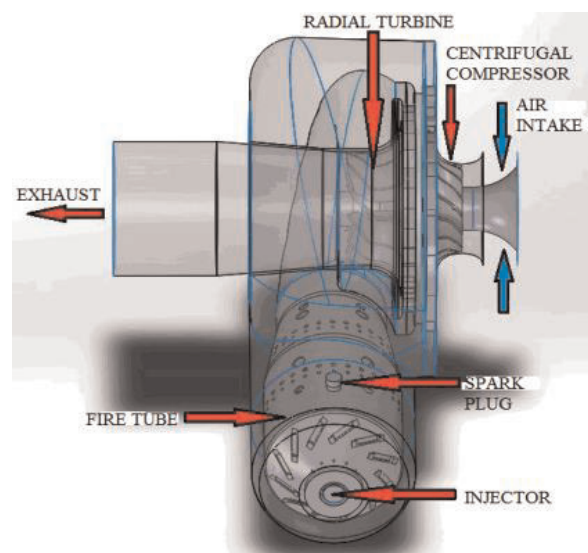


Figure 9.
Garrett micro gas turbine geometry.

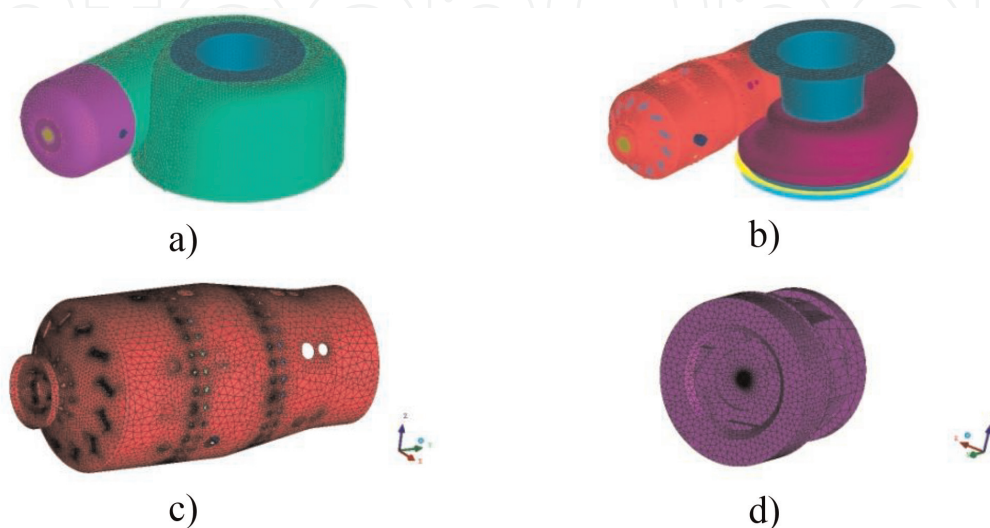


Figure 10.
Computational grid: (a) the exterior of the combustion chamber assembly, (b) the interior of the combustion chamber assembly, (c) the fire tube, (d) the injector.

The nominal functioning regime (20 KW load) has been considered for the simulation; thus, the fuel mass flow rate has been set at 0.0075 kg/s, and the air mass flow has been set at 0.522 kg/s. The air excess is of 4.7. Generally, for a gas turbine engine, the excess air should be between 3 and 5 [1]. The initial air temperature was set at 420 K. The used liquid fuel, Jet A, has been considered to enter the computational domain in the form of droplets. The mean diameter of the droplets has been assumed to be 30 μm , a value chosen based on the liquid droplet distribution diagram. The initial fuel temperature has been set at 300 K. The fuel spray cone angle has been set at 70° , based on the data presented in the micro gas turbine's maintenance manual [13].

A Reynolds averaged Navier-Stokes (RANS)-type turbulence model has been chosen, namely, the $k-\epsilon$ model, which is a numerically stable and robust model and very popular in the realization of technical applications numerical simulations [14–17].

The chosen combustion model has been the EDM model, based on a two-step kerosene-air reaction mechanism, imported from the ANSYS library. A simple reaction mechanism has been chosen because the purpose of these numerical simulations was to see if the used numerical models give a good approximation of the turbo engine functioning as a whole. The pollutant emission level has not been of interest at this stage. Using a more complex reaction mechanism would have been more time-consuming and would have required more powerful computational resources. The EDM combustion model has been chosen because of its simplicity and robust performance in predicting turbulent reacting flows. Because of these, the model is very often used in the realization of technical application numerical simulations [18–21].

The fuel droplet atomization and evaporation processes have been simulated using the cascade atomization and breakup (CAB) model, respectively, and the liquid evaporation model, both models imported from ANSYS library.

The reference pressure has been set at 101,325 Pa.

In **Figure 11** the pressure field through the micro gas turbine is presented. The pressure levels are relative to the reference pressure.

The pressure inside the fire tube is quasi-constant, as it can be seen in **Figure 3**, thus conforming the hypothesis that the combustion process inside a gas turbine combustion chamber takes place at constant pressure. The average air absolute total pressure at compressor exit-combustion chamber entrance is 275.466 Pa, thus obtaining an overall compression ratio of 2.7:1 which is close to the reported overall compression ratio of 3:1. The obtained pressure loss through the combustion chamber assembly is of 15%.

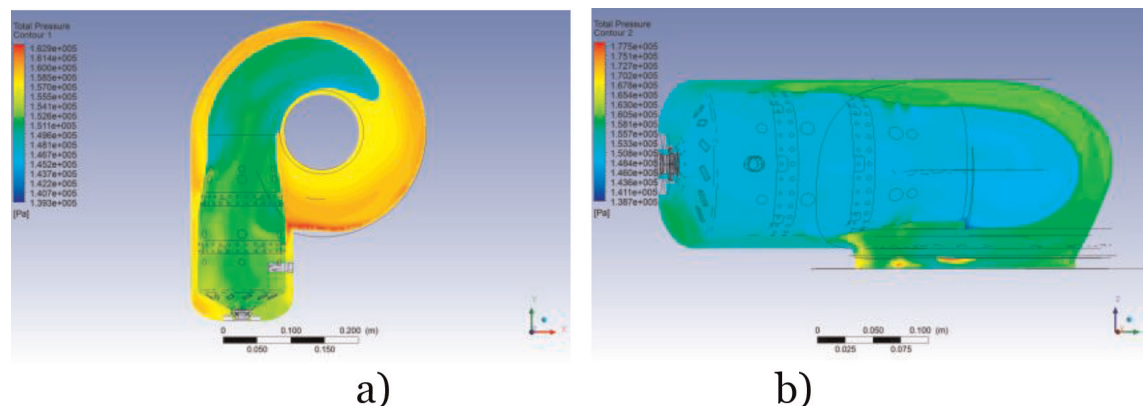


Figure 11.
The total pressure field inside the combustion chamber assembly: (a) plan XY and (b) plan YZ.

In **Figure 12** the total temperature field through the micro gas turbine is presented.

From **Figure 12(a)** it can be observed that high-temperature zone is found only inside the fire tube and does not extend into the volute that redirects the exhaust gases to the turbine stator. The average total temperature at combustion chamber exit-turbine entrance is 992 K.

In **Figure 13** the fuel spray cone and the fuel droplet diameter distribution are presented.

From **Figure 13** it can be observed that the fuel is completely evaporated in the primary zone of the fire tube, before reaching the walls. This confirms that the numerical models chosen to simulate the spraying and vaporization processes of the liquid fuel are appropriate for the given application.

In **Figure 14** Jet A vapor mass fraction field is presented.

The results presented in **Figures 13** and **14** are in good correlation. Jet A vapors obtained from the vaporization of the liquid fuel are located in the primary zone of the fire tube. They are completely consumed inside the fire tube, as it should happen in the case of a properly functioning turbo engine. The average Jet A vapor mass fraction at combustion chamber assembly exit is of 7×10^{-7} .

In **Figures 15** and **16**, the CO mass fraction field and the CO₂ mass fraction field, inside the combustion chamber, are presented, respectively.

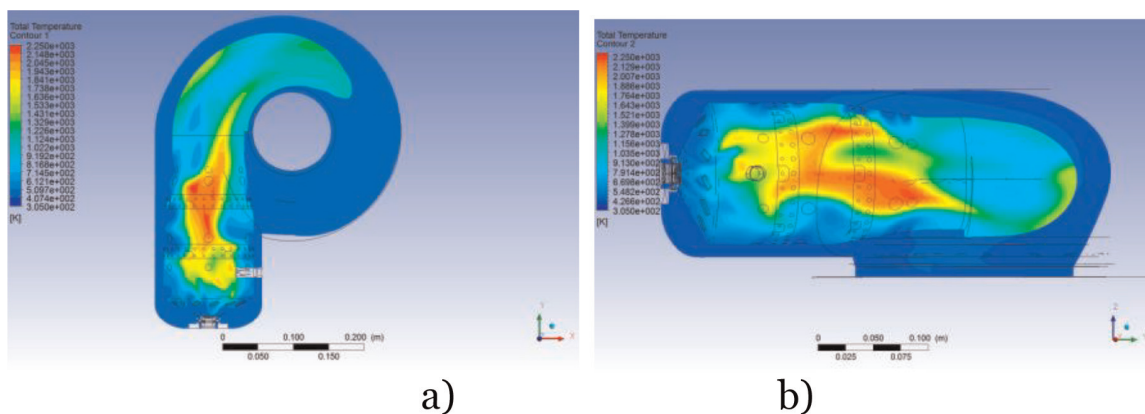


Figure 12.
The total temperature field inside the combustion chamber assembly: (a) plan XY and (b) plan YZ.

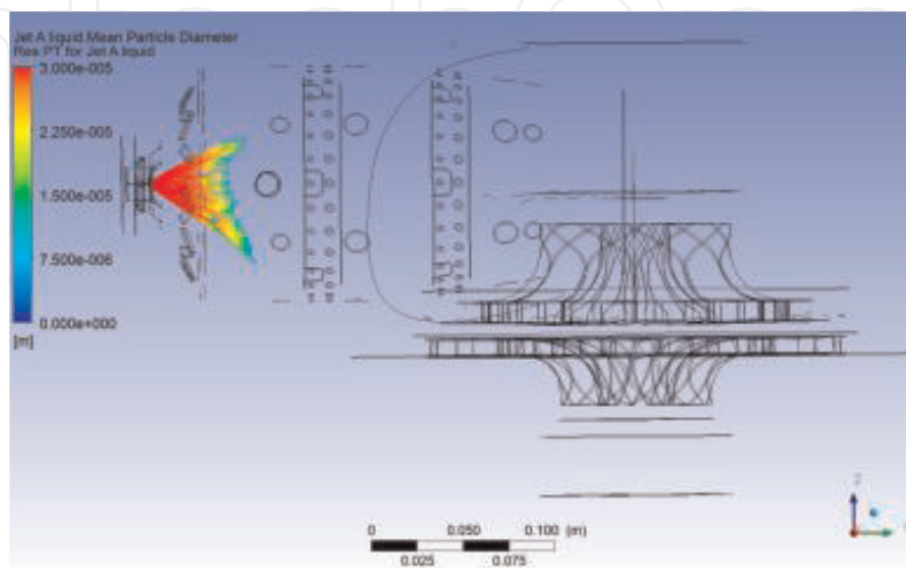


Figure 13.
Fuel spray cone and droplet diameter distribution.

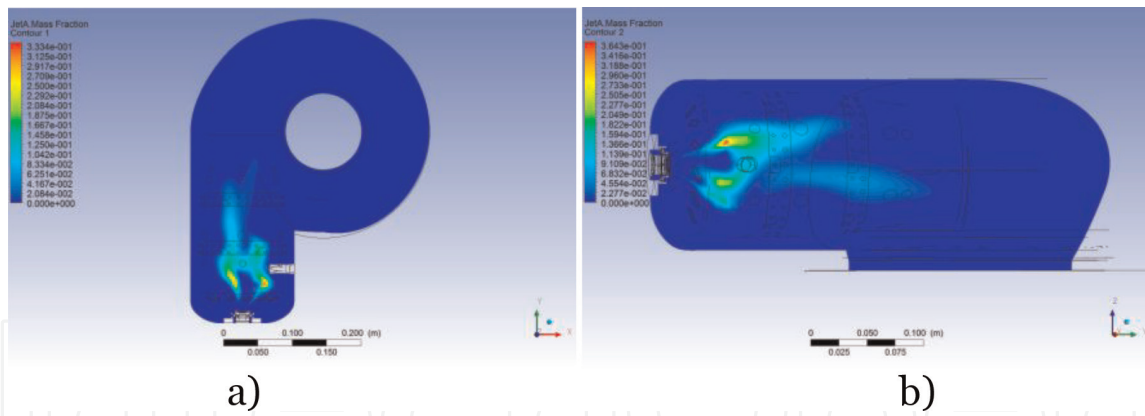


Figure 14.
Jet A vapor mass fraction field: (a) plan XY and (b) plan YZ.

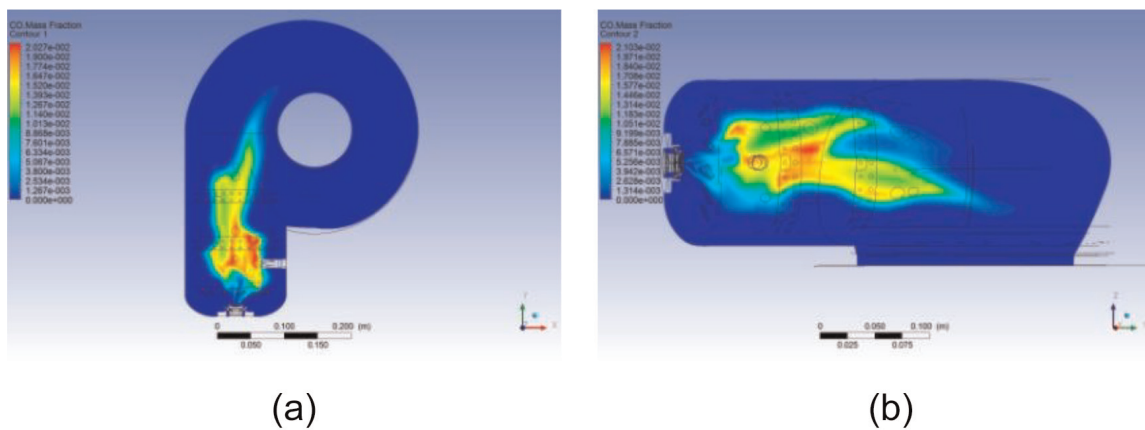


Figure 15.
The CO mass fraction field: (a) plan XY and (b) plan YZ.

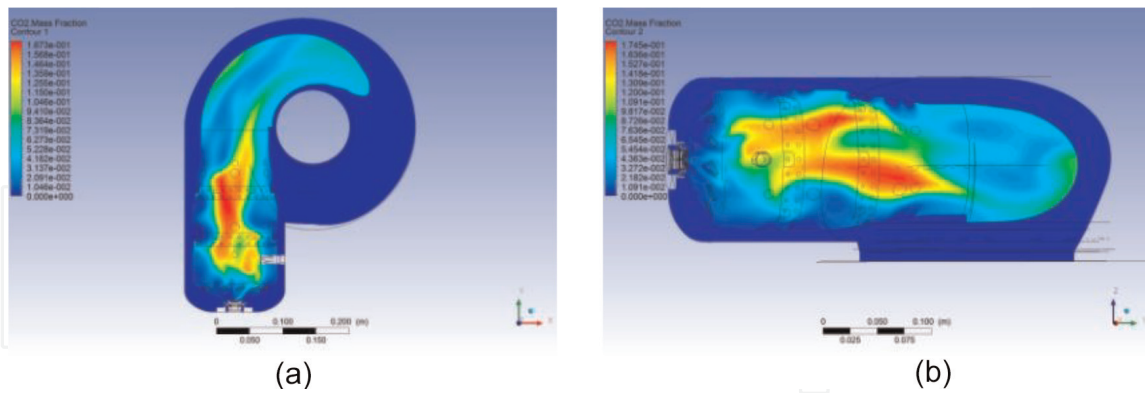


Figure 16.
The CO₂ mass fraction field: (a) plan XY and (b) plan YZ.

The highest CO and CO₂ concentrations are found inside the fire tube. This is in good correlation with the temperature field (**Figure 12**) and Jet A vapor field (**Figure 14**), suggesting that the combustion reaction takes place and is completed inside the fire tube. The average CO and CO₂ mass fractions at combustion chamber assembly exit are 7.4×10^{-6} and 0.046532, respectively.

Based on the obtained results, the temperature and pressure fields, the fuel vapor, and CO and CO₂ mass fraction fields, it has been concluded that the numerical models used for the numerical simulation of the gas-thermodynamic processes inside the combustion chamber are appropriate for the given application, the results being consistent with actual functioning data of the Garrett micro gas turbine.

3.3 Afterburning system

The afterburning system is a component that is added to aviation engines (gas turbine engines), usually military ones, in order to maximize the thrust force of the planes. But it also has industrial applications like cogeneration. Cogeneration is a modern solution which allows simultaneous production of electricity and heat. Due to cogeneration units, not only it is possible to lower the costs associated with heating and electricity producing, but it can also generate it in a way that is efficient and environmentally friendly. The fact that the combustion process in the gas turbine consumes only a small part of the oxygen from the intake air flow makes possible the application of a supplementary firing (afterburning) for increasing the steam flow rate of the heat recovery steam generator. A new patented afterburner installation was proposed, for use in cogenerative applications (**Figure 17**) [22].

This study focuses on Stage I of the afterburner (**Figure 18**) for which a special experimental installation was designed. Here experimental measurements and numerical results of mean velocity and temperature are presented. The velocity measurements are carried out using particle image velocimetry (PIV), and the temperature measurements are performed using Rayleigh spectroscopy. Supplementary, flame front position measurements are presented, obtained with the planar laser-induced fluorescence (PLIF) technique [23]. The experimental setup, closely reproduced by the numerical simulations, consists of a post-combustion system, designed and manufactured at COMOTI and installed behind a Garrett 30–67 gas turbine engine serving as a gas generator. The flame is stabilized by means of a V-shaped flame holder, placed in the gas generator exhaust flow. Methane is injected into the flow upstream of the flame holder and ignited downstream of it, at a location where premixed conditions are reached.

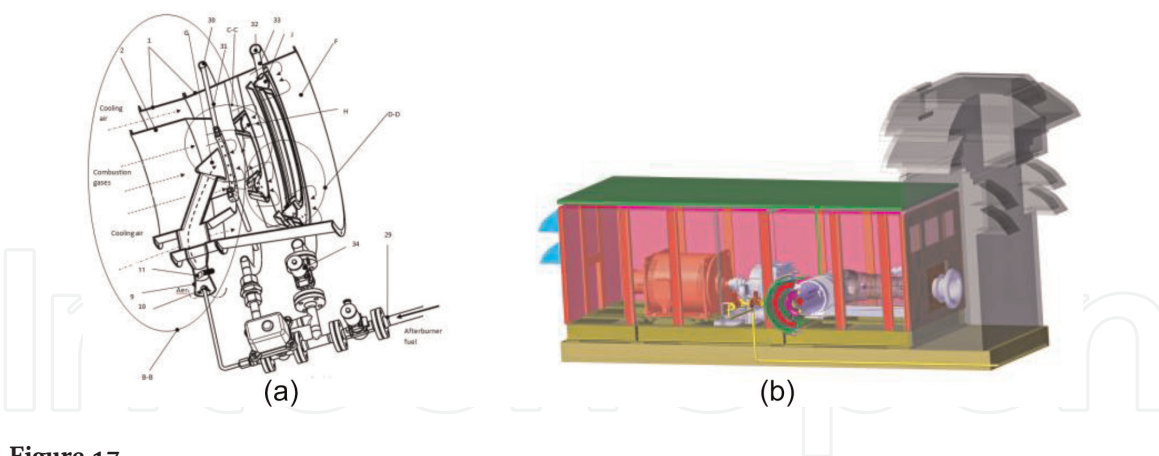


Figure 17.
Afterburning system for cogeneration: (a) partial 3D viewing and (b) assembly of the installation.

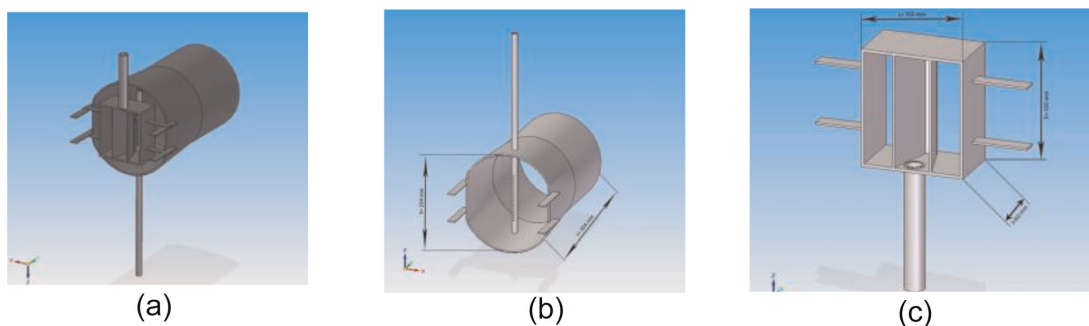


Figure 18.
Experimental setup design: (a) afterburner; (b) casing; and (c) flame stabilizer.

3.3.1 Experimental setup

3.3.1.1 The afterburning system

The afterburning system, shown in **Figure 18**, has the following overall dimensions: length = 304 mm, height = 228 mm, and width = 168 mm. The afterburning system is composed of a casing and flame stabilizer assembly. The casing has 240 mm in height and 304 mm in length. The casing also includes a gas fueling pipe with the following dimensions: diameter = 10 mm and height = 470 mm. The gas pipe has 20 equally spaced holes of 2 mm in diameter. The flame stabilizer assembly includes the actual, “V”-shaped flame stabilizer. The assembly also includes the ignition pipe, of the following dimensions: diameter = 16 mm and height = 115 mm. The post-combustion system presented above can raise the exhaust gas temperature up to a temperature of maximum 1800 K.

3.3.1.2 The gas turbine engine Garrett 30-67

The gas turbine engine Garrett 30-67 [24] was fitted with a pipe that allows PIV flow seeding and transfers the seeded exhaust gas to the afterburning system (**Figure 19**).

3.3.1.3 The PIV measurement system

The experimental program presented here aimed at determining the instantaneous three-dimensional velocity field in the exhaust gas downstream of the post-combustion system. For the measurement a medium intensity laser beam was used, emitted by a Nd:YAG double-pulsed laser (Litron Lasers, wavelength of 532 nm and a maximum output power of 1200 mJ), simultaneously with the triggering of two fast charge-coupled device (CCD) cameras that record the images thusly formed. The laser beam is passed through a light sheet optic device that converts the beam to a light sheet in the experimental zone. The time interval between two laser impulses was of 10 μ s [25].

3.3.1.4 Rayleigh spectroscopy

Rayleigh scattering (RS) is a nonresonant elastic effect in contrast to the commonly used laser-induced fluorescence. RS is instantaneous and therefore completely independent of the molecules' environment [26].

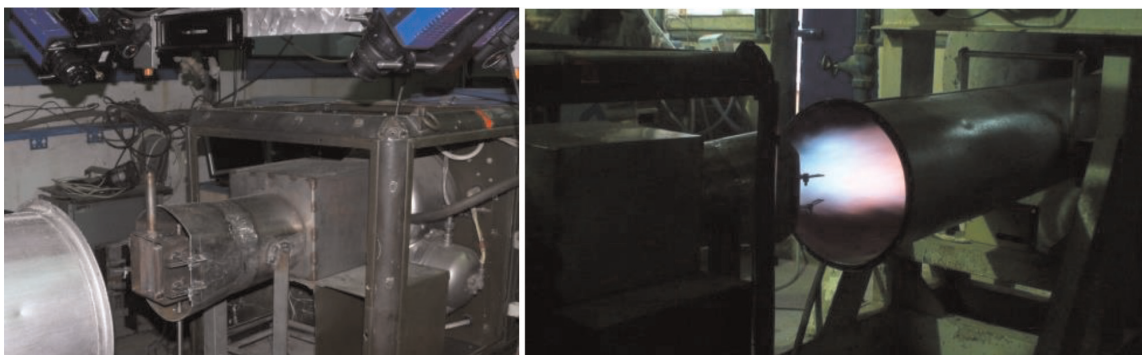


Figure 19.
Experimental setup.

3.3.1.5 The PLIF measurement system

The planar laser-induced fluorescence method is presented here. When laser radiation is tuned to specific wavelengths, it will excite certain species (molecules) within a flame to a higher energy level. Fluorescence occurs when this excited state decays and emits radiation of a longer wavelength than the incident laser radiation. In the atmospheric pressure flame created by the afterburner, quenching is negligible, and the fluorescence signal is proportional to the OH concentration. For the OH measurements presented here, the coumarin 153 dye was used. Laser light has a fundamental frequency of 1064 nm. The fluorescent light photons are captured by an intensified charge-coupled device (ICCD) camera equipped with a filter that lets through only the fluorescent light wavelength [23].

3.3.1.6 CFD software and numerical simulation setup

In order to evaluate the effect of the combustion model validity on the accuracy of the numerical simulation, the reference numerical simulation will use an extended EDM [27] combustion model, implemented in a fully three-dimensional numerical simulation conducted using the commercial software ANSYS CFX. In this study, the shear stress transport (SST) model has been used. The computational domain includes the post-combustion system described in the previous section and extends 350 mm downstream of the bluff body stabilizer. In the transversal direction, the extension measures 300 mm, centered on the post-combustion symmetry axis, and in the spanwise direction, it reaches the edges of the post-combustion chamber.

The following results will be shown. Combustion temperature has a significant effect on NO_x . NO emissions increase, but N_2O emissions decrease, with increasing temperature. Velocity—the speed at which premixed laminar and turbulent flames propagate—is a fundamental parameter in many combustion applications, such as engines and gas turbines. Flame speeds influence knocking events in spark-ignited engines and play an important role in their performance and emissions. OH concentration shows flame front shape and stability. **Figures 4 and 5** present, respectively, the mean temperature and velocity components along the symmetry axis of the afterburner. The length of the recirculation region that is created in the flow by the presence of the bluff body stabilizer is of about 90 mm, and the maximum absolute value of the negative velocity reaches about 25 m/s. The far-field free stream velocity is about 35 m/s.

In **Figures 20–23**, various comparisons between numerical and experimental results are presented.

The mean velocity field of the flow inside the previously defined computational domain and its axial and transversal components are presented.

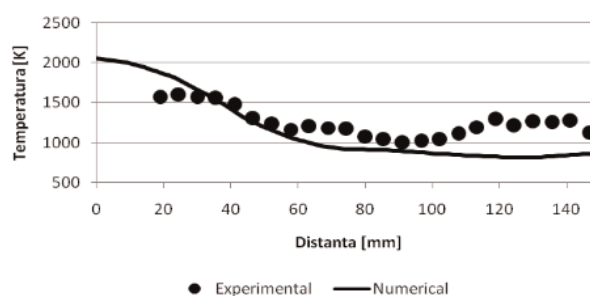


Figure 20.
Temperature profile along the centerline.

Below the variation of the mean OH concentration along the axis of symmetry is presented. The reaction mechanism used in numerical simulation did not allow the concentration of hydroxyl (OH) to be captured so that it is presented experimentally and not numerically validated. It must be noted from the beginning that the OH radical is a very fast radical, which is created and destroyed rapidly in the combustion process. For this reason, its presence can be detected in the flame front only, being a very precise indication on its position. As seen in **Figure 24**, the position of the mean flame front coincides to the recirculation region that forms downstream of the flame stabilizer. The turbulent flame brush, clearly visible in **Figure 24**, determines a significant increase of the mean flame front, as compared to its instantaneous thickness. The turbulent flame brush is an effect of the turbulent intermittency, which causes, through the effect of the turbulent fluctuation of the flame, a given point in space in the flame front region to be part of the time inside the flame front and part of the time outside it. Therefore, the averaging

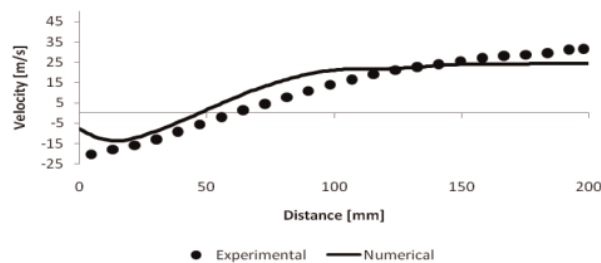


Figure 21.
Axial velocity profile along the centerline.

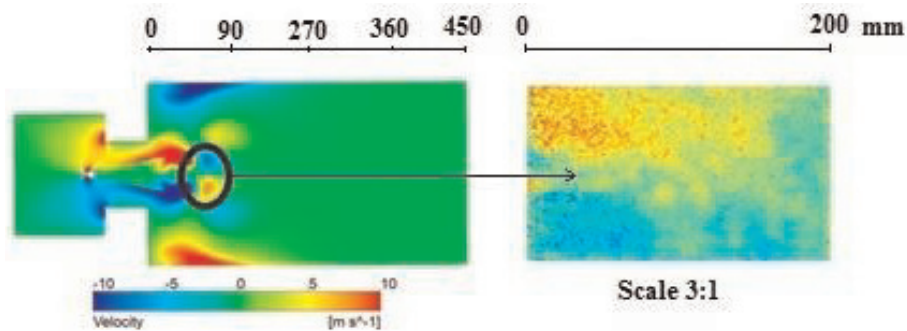


Figure 22.
Left: numerical mean axial velocity field. Right: PIV experimental mean axial velocity field (the same velocity color scale).

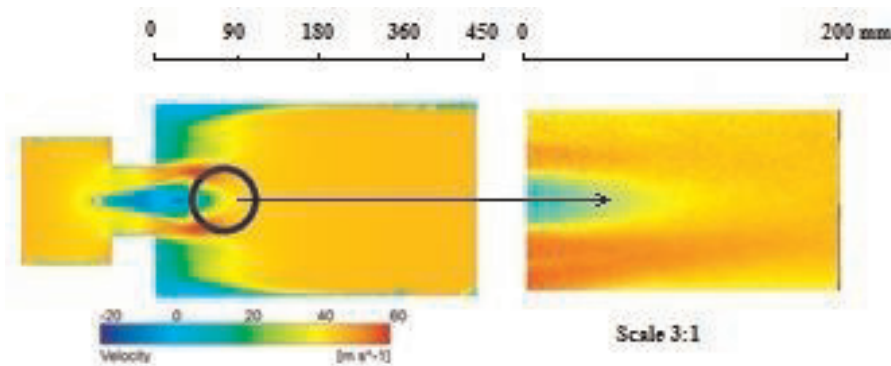


Figure 23.
Left: numerical mean transversal velocity field. Right: experimental mean transversal velocity field (the same velocity color scale).

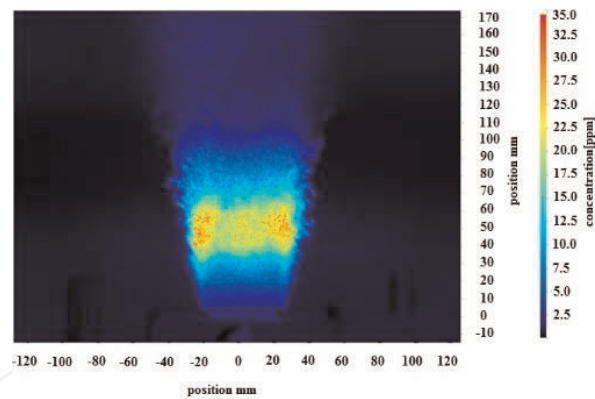


Figure 24.
Mean OH axial concentration.

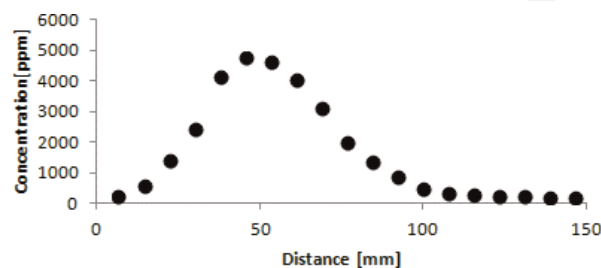


Figure 25.
The variation in the mean OH concentration along the axis of symmetry.

process leads to a region much thicker than the very thin flame front characteristic to a laminar flame, where the mean fields have characteristics corresponding partially to the flame front, partially to the preheating region, and partially to the oxidation zone [28]. In the axial direction in **Figure 25**, the maximum OH concentration, of about 5000 ppm, is reached at about 50 mm from the flame stabilizer trailing edge, and the turbulent flame brush extends between 0 and 100 mm with respect to the same axial coordinate origin.

3.4 Hydrogen use in gas turbines

Hydrogen is studied as a possible fuel in gas turbines due to its high calorific value and promising results in the field of environmental protection. More, hydrogen become actual again, since new ways for producing and transporting it developed lately. One interesting idea is to produce the hydrogen on site by electrolysis, using wind power or solar energy, and to transport it using the existing natural gas distribution network. Combining hydrogen with natural gas strongly influences the combustion parameters, due to the different properties of the mixture. Using the existing equipment would face new problems, like the modification of the flame front, the risk of flashback, and higher temperatures.

By numerical simulation on the combustion chamber of a small gas turbine, for 100% CH₄ and 100% H₂, a clear difference can be observed in **Figure 26**, indicating probable working problems and a possible installation's component damage.

Thus, the idea of searching for a new solution was born, by changing the type of injector and part of the geometry of the combustion chamber.

In the process of designing of the new injector solution, numerical simulations were used, testing and comparing different types, in order to obtain an optimized variant to be produced and experimentally tested later on. For example, in **Figure 27**, two types of geometries for swirl injectors were compared in respect to the flow characteristics and temperature and velocity fields.

The second type of injector shows better volume flame repartition and more intense recirculation zones, benefic characteristics for flame stability, and pollutant emission formation/inhibition. Also the higher swirl number resulted for type 2 is promising, influencing the inlet turbulence, with the mention that other authors of [30] suggest that it is not the case that a rise in the swirl number leads always to an increase in combustion efficiency, but there is an optimum angle for swirling vanes at which the combustion efficiency, temperature, and radiation heat transfer of the flame stand at their maximum. In the same time, the higher local temperatures can

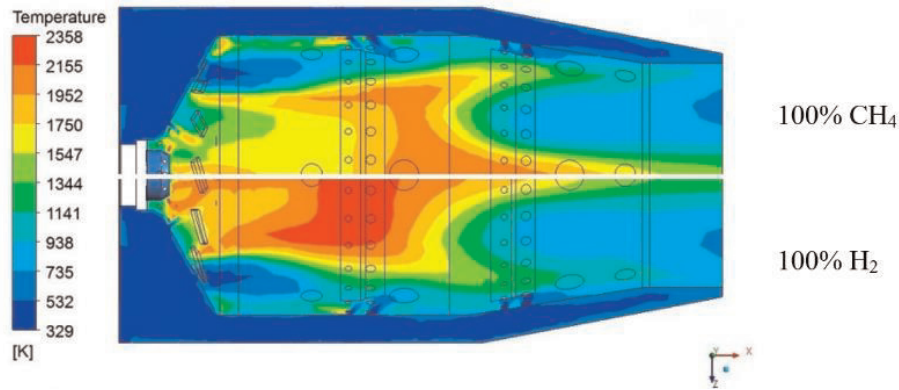


Figure 26.
Temperature field distribution for CH_4 and H_2 combustion.

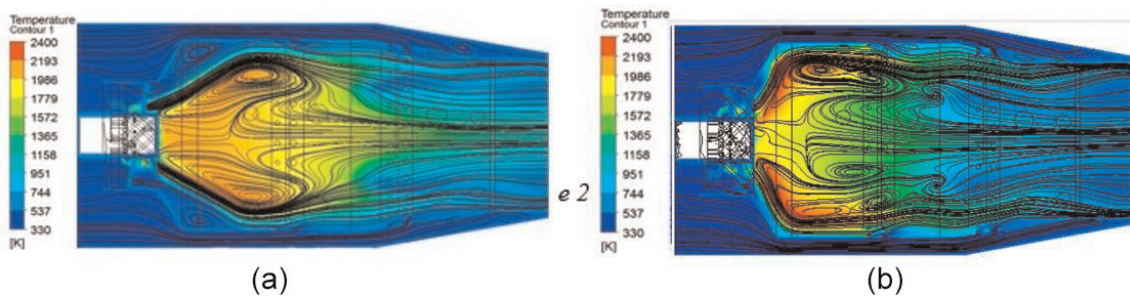


Figure 27.
CFD analysis for two different types of swirled injectors [29]. (a) Type 1 and (b) Type 2.

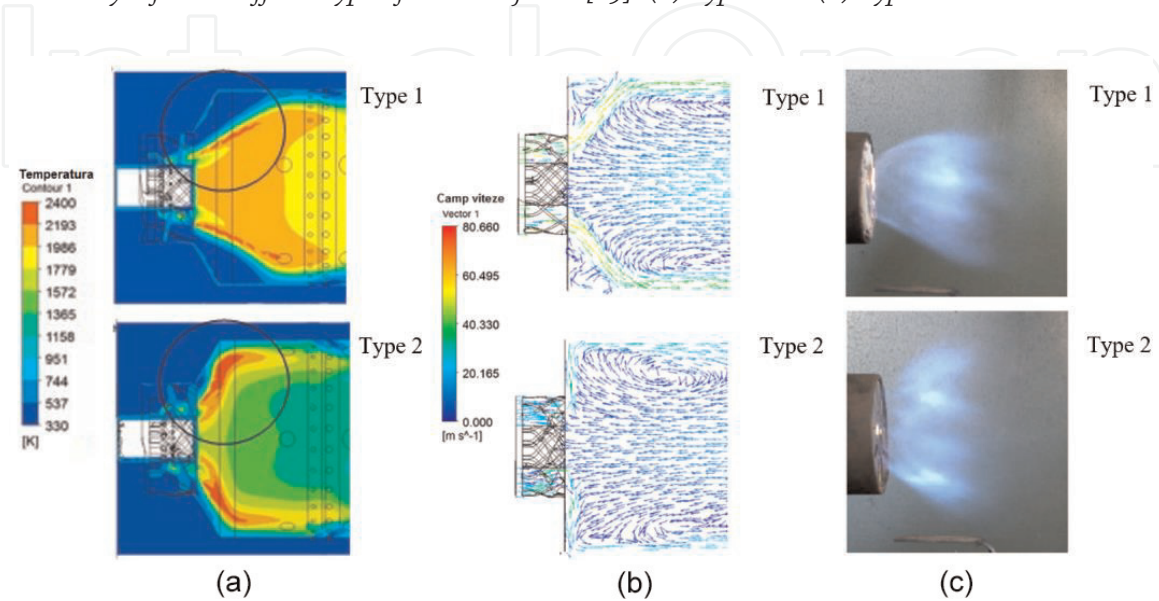


Figure 28.
Comparison of CFD results and visualization during the experiment. (a) Temperature field (combustion simulation); (b) velocity fields (cold simulation); and (c) experimental images.

lead to thermal NO_x formation, a disadvantage that can be controlled by flame cooling technics.

The CFD results show a clear picture of the differences between the two types, with very similar results to the later conducted experiments (**Figure 28**), helping in choosing the right geometry and leading to the optimized version to be manufactured and tested (**Figure 29**) [31].

The design of the new swirl injector was patented, considering some innovative ideas. For example, the convergent shape of the nozzle avoids the uneven velocities between the base section and tip section at the exit of the channel and leads to higher velocity in the exit section than the burning velocity of the fuel, eliminating the danger of flashback phenomenon.

The specific numerical simulation methods also helped for studying the main subject of the work, mentioned above, focusing on the different aspects of combustion of the mixtures $\text{CH}_4\text{-H}_2$, with various volumetric proportions (**Figure 30**). The results show relevant data, with very similar results as in the experiments,

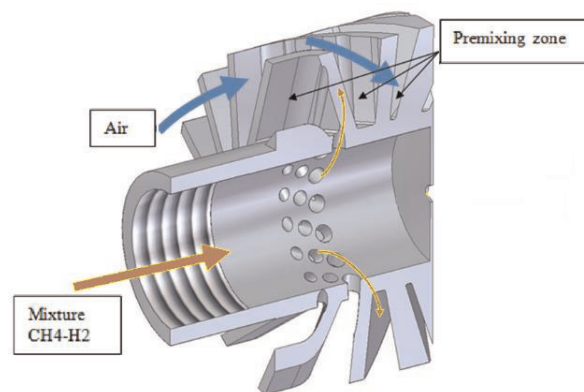


Figure 29.
The swirl injector and working principle [29].

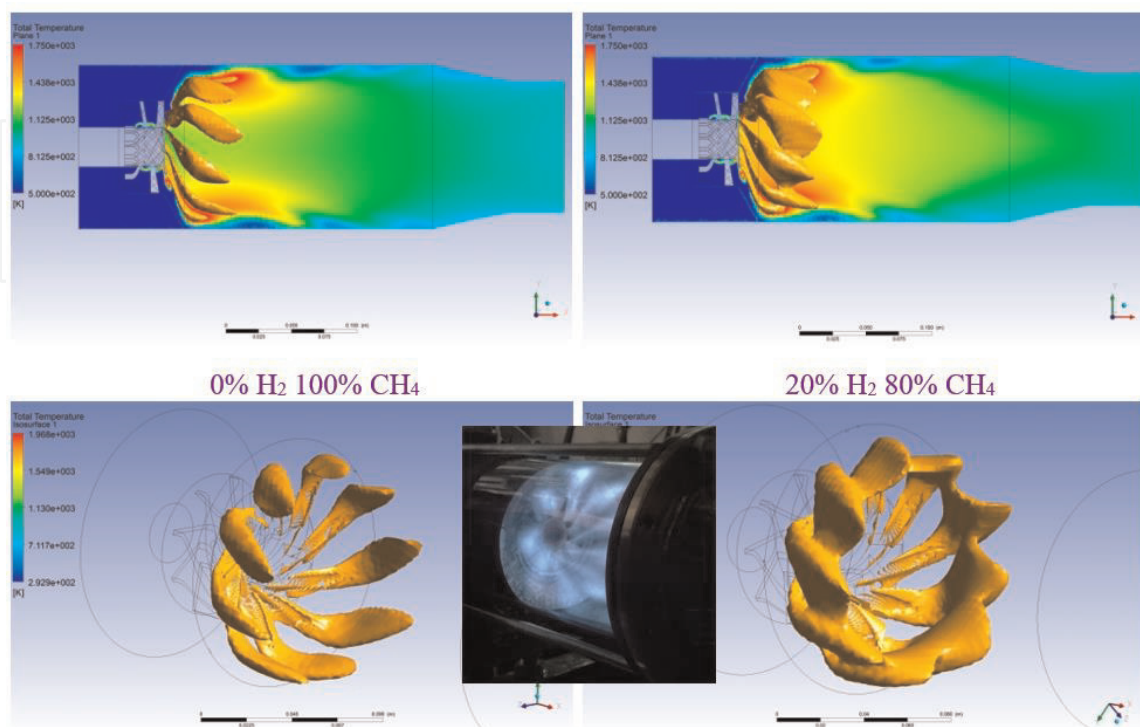


Figure 30.
Isometric section for 0% H_2 and 20% H_2 (airflow 0.04 kg/s, excess air 3.5).

validating the chosen CFD methods and input values, as part of a PhD. thesis [32] and part of a Romanian Research Authority-funded project [33].

For all these RANS simulations, $k-\varepsilon$ model turbulence model was used. As for combustion model, the flamelet probability density function (FPDF) model was chosen, because of the CFX available kinetic reaction library, which provided a fast and easy way to mix the two gaseous fuels. This mathematical model has some known drawbacks too, like slightly higher temperature estimations and the absence of NO_x calculation, but this case did not require high precision; the only purpose was just getting a correct image of the combustion process for different cases, in order to optimize the solution and to have a clear preview to the experimental phase.

For this specific case, the combustion of $\text{CH}_4\text{-H}_2$ mixtures, there is also an interesting important issue that has no solution for the moment: the existing mathematical models do not take into consideration the very different reaction times of the two fuels in this mixture and thus cannot capture and validate the hypothesis that the hydrogen from the mixture burns faster and consumes at a higher rate from the oxygen required to burn the entire mixture, thus resulting in incomplete combustion of methane.

Considering all these aspects, depending on the studied case and on the purpose of the research, different CFD methods should be chosen, considering the resources, the allocated time, and the requested detail level of the results.

4. Conclusions

CFD represents a powerful tool that can be used even for studying the complex process taking place into the combustion chamber of a gas turbine. There exist many simple models giving relatively good results since of main interest in this field is the combustion temperature which is a measure of the entire gas turbine performance. Still, if someone needs to predict the pollutant emissions, complex models including reaction mechanisms must be employed.


The given examples show that good correlation can be obtained between CFD simulations and experiments at gas turbine assembly level, no matter the size of the gas turbine nor the fuel. An afterburning application was also analyzed since higher velocities are expected, but the results are still conclusive.

Author details

Valeriu Vilag*, Jeni Vilag, Razvan Carlanescu, Andreea Mangra and Florin Florean
COMOTI Romanian Research and Development Institute for Gas Turbines,
Bucharest, Romania

*Address all correspondence to: valeriu.vilag@comoti.ro

IntechOpen

© 2019 The Author(s). Licensee IntechOpen. This chapter is distributed under the terms of the Creative Commons Attribution License (<http://creativecommons.org/licenses/by/3.0>), which permits unrestricted use, distribution, and reproduction in any medium, provided the original work is properly cited. 

References

- [1] Boyce M. Gas Turbine Engineering Handbook 4th Edition, Hardcover ISBN: 9780123838421, eBook ISBN: 9780123838438, Imprint: Butterworth-Heinemann. 2011
- [2] Jeni VP. Contributions regarding the utilization of alternative fuels in reusable aviation gas turbines [PhD. thesis]. Bucharest: Politehnica University of Bucharest; 2013
- [3] The jet engine, Rolls Royce 1996
- [4] Clean Sky. Available from: www.cleansky.eu
- [5] Lefebvre AH, Ballal DR. Gas Turbine Combustion. Alternative Fuels and Emissions. 3rd ed. New York: CRC Press; 2010
- [6] Pimsner V, Vasilescu CA, Radulescu GA. Energetica Turbomotoarelor cu Ardere Interna. București: Editura Academiei Republicii Populare România; 1964
- [7] Peters N. Turbulent Combustion. Cambridge, UK: Cambridge University Press; 2000
- [8] Peters N. Product-Manual for ANSYS CFX v16. ANSYS INC, Released 13.0. 2015
- [9] Porumbel I. Large Eddy Simulation of Bluff Body Stabilized Premixed and Partially Premixed Combustion. Atlanta: Georgia Institute of Technology; 2006
- [10] Popescu J, Vilag V, Petcu R, Silivestru V, Stanciu V. Researches Concerning Kerosene-to-Landfill Gas Conversion for an Aero-derivative Gas Turbine, ASME Turbo Expo 2010: Power for Land, Sea and Air; 14–18 Iunie 2010; Glasgow, UK. NEW YORK, USA: ASME. ISBN: 978-0-7918-3872-3
- [11] ANSYS CFX Help
- [12] Petcu AC. Research regarding the use of camelina vegetable oil as fuel [PhD. thesis]. Bucharest: Politehnica University of Bucharest; 2016
- [13] Petcu AC. Technical Manual Shaft Power Gas Turbine Engine model GTP 30-67
- [14] Dumitrescu O, Gherman BG, Porumbel I. Importance of a second entrance in a test cell. INCAS Bulletin. 2018;10(1):63-72
- [15] Carlanescu R, Prisecaru T, Petcu AC, Porumbel I. Numerical analysis of the effect of the fuel composition on the flame characteristics in hydrogen methane diffusion flames. In: International Conference on Jets, Wakes and Separated Flows; Stockholm. 2015
- [16] Petcu AC, Sandu C, Berbente C. Numerical simulations of jet-A combustion in a gas turbine combustion chamber. International Journal of Engineering and Innovation Technology. 2013;3(2):487-491
- [17] Carlanescu R, Prisecaru T, Mangra A, Kuncser R, Florean F, Enache M. The analysis of the combustion of premixed methane-hydrogen mixtures stabilised by an inovative swirl injector. In: 10th Mediterranean Combustion Symposium; Naples, Italy. 2017
- [18] Gherman B, Malael I, Florean FG, Porumbel I. Experimental combustion chamber simulation at transient regimes. In: E3S Web of Conferences 85. 2019
- [19] Florean FG, Gherman BG, Porumbel I, Carlanescu R, Dumitrascu G. Experimental measurements and numerical simulations in bluff body stabilized flames. In: 1st International Conference

New challenges in Aerospace Sciences
NCAS 2013; November 7–8, 2013;
Bucharest, Romania

[20] German BG, Florean FG, Carlanescu C, Porumbel I. On the influence of the combustion model on the result of turbulent flames numerical simulations. In: ASME Turbo Expo 2012. Combustion, Fuels and Emissions, Copenhagen, Denmark. Vol. 2. 2012

[21] Petcu AC, Gherman B, Florean FG, Sandu C, Porumbel I. Numerical simulations of round turbulent jet flames. In: Starik AM, Frolov SM, editors. Nonequilibrium Processes in Plasma, Combustion and Atmosphere. Moscow: Torus Press; 2012. ISBN 978-5-94588-121-1

[22] Patent number 128845A0, Florean FG, Petcu AC, Carlanescu R, Porumbel I, Sandu C, Carlanescu C. Multistage afterburner installation in a self-ventilated turboengine skyd. Official Bulletin of Industrial Property no. 7/2016

[23] LaVision GmbH. Product-Manual for DaVis 7.2 "LIF in Gaseous Fluids", Anna-Vandenhoeck-Ring 19, D-37081 Göttingen. 2009

[24] Florean F. Research on the afterburner systems using gas fuels [PhD thesis] S.L.: "Gheorghe Asachi" Technical University of Iasi, Faculty of Mechanics; 2013

[25] LaVision GmbH. "Product-Manual for PIV", Anna-Vandenhoeck-ring 19, D-37081 Göttingen. 2009

[26] LaVision GmbH. "Product-Manual for DaVis 7.2, Rayleigh Thermometry", LaVision GmbH, Anna-Vandenhoeck-Ring 19, D-37081 Göttingen. 2009

[27] Florean FG, Popescu JA, Porumbel I, Carlanescu C, Dumitrascu G. Experimental measurements and numerical simulations in isothermal

turbulent flows, GT2012-69377. In: Proceedings of the ASME TURBO EXPO 2012. Vol. 1: Aircraft Engine; Ceramics; Coal, Biomass and Alternative Fuels; Controls, Diagnostics and Instrumentation. 2012. pp. 283-292. DOI: 10.1115/gt2012-69377

[28] Florean FG, Porumbel I, Carlanescu C, Dumitrascu G. LIF experiments in a turbulent reactive flow using an afterburner. In: 4th CEAS Air and Space Conference–Innovative Europe, Linköping, Sweden, September 16–20, 2013, Proceedings. pp. 878-884

[29] Carlanescu R, Prisecaru T, Prisecaru M, Soriga I. Swirl injector for premixed combustion of hydrogen–methane mixtures. s.l.: Journal of Energy Resources Technology. 2018;140(7). Paper No: JERT-16-1506. DOI: 10.1115/1.4039267

[30] Pourhoseini SH, Asadi R. An experimental study of optimum angle of air swirler vanes in liquid fuel burners. ASME Journal of Energy Resources Technology, 2016;139(3). Paper No: JERT-16-1147. DOI: 10.1115/1.4035023

[31] Carlanescu R, Prisecaru T, Kuncser R, Pop EA. The optimization of a swirl injector for combustion of hydrogen fuel mixtures. U.P.B. Scientific Bulletin, Section D: Mechanical Engineering. 2018. ISSN 1223-7027

[32] Carlanescu R. Numerical and experimental research on the effects of hydrogen mixing with natural gas in the combustion chamber of a gas turbine [PhD thesis]. Bucharest: Politehnica University of Bucharest; 2019

[33] COMOTI. Romanian Research and Development Institute for Gas Turbines, "Combustion Chamber with Hydrogen-Natural Gas Mixture Fuel", Romanian Government founded research program, name HIDROCOMB, Contract UEFISCDI no. 76/2014